Global Environmental Science
www.sciltp.com/journals/ges

*Article*

# Microbial Response to Mining, Dressing and Smelting Activities in Antimony-Mining Area: Insights into C, N, S and As Cycling

Weisong Pan [1], Boyan Zhang [1], Chuan Wu [2,3], Yayuan Huang [2,*], Xiaoran Xiong [1], Yahui Wu [2], Tsang Po Keung [3] and Waichin Li [3,*]

[1] College of Bioscience and Biotechnology, Hunan Agricultural University, Changsha 410128, China
[2] School of Metallurgy and Environment, Central South University, Changsha 410083, China
[3] Department of Science and Environmental Studies, The Education University of Hong Kong, Hong Kong SAR, China
* Correspondence: yyhuang@csu.edu.cn (Y.H.); waichin@eduhk.hk (W.L.)

**How To Cite:** Pan, W.; Zhang, B.; Wu, C.; et al. Microbial Response to Mining, Dressing and Smelting Activities in Antimony-Mining Area: Insights into C, N, S and As Cycling. *Glob. Environ. Sci.* **2026**, *2*(2), 193–207. https://doi.org/10.53941/ges.2026.100013

## Publication History

Received: 22 December 2025
Revised: 26 March 2026
Accepted: 17 April 2026
Published: 15 May 2026

## Keywords

mining; dressing and smelting; metagenome; arsenic; antimony

## Highlights

- Mining soils showed the lowest diversity and stronger sulfur oxidation.
- Dressing soils were characterized by enhanced iron-related respiration.
- Smelting soils enriched genes for N cycling, S metabolism and As/Sb resistance.
- Core taxa linked C, N, S and As/Sb cycling across all processing stages.

**Abstract:** Arsenic (As) and antimony (Sb) are toxic metalloids with similar physicochemical properties, and their microbial transformation is closely linked to carbon (C), nitrogen (N), and sulfur (S) cycling. Mining-related anthropogenic activities substantially alter the bioavailability of As/Sb and microbial metabolism, but the specific impacts of sequential mining, dressing, and smelting processes on microbial communities and C, N, S, and As/Sb cycling remain unclear. In this study, we systematically investigated soil physicochemical properties, microbial communities, and functional potentials in an abandoned Sb mine area. The results showed that different mineral processing stages significantly altered soil nutrient status and heavy metal distribution, and induced distinct shifts in microbial diversity, composition, and metabolic potential. The mining area exhibited the lowest bacterial α-diversity, whereas the smelting area supported the highest diversity. Metal-tolerant taxa, including *Proteobacteria*, *Actinobacteria*, and *Firmicutes*, were enriched in the mining area, with dominant genera such as *Pseudomonas*, *Bacillus*, and *Bradyrhizobium*. Functional analyses indicated clear stage-specific differentiation of microbial metabolism: the dressing area was characterized by enhanced iron-related respiratory potential, the smelting area by increased methyl compound utilization, and the mining area by stronger sulfur oxidation and organic matter degradation potential. Metagenomic analysis further revealed that the reductive citric acid cycle was the dominant carbon fixation pathway, while smelting activities increased the relative abundance of genes involved in nitrate transformation, sulfur metabolism, and As/Sb resistance. Core taxa including *Streptomyces*, *Sphingopyxis*, *Sphingomonas*, and *Pseudomonas* were broadly associated with C, N, S, and As/Sb cycling across all sites. This study provides new insights into how sequential mining, dressing, and smelting activities shape microbial community assembly and biogeochemical functions in metalloid-contaminated soils. The findings have broader relevance for understanding microbial adaptation and for developing site-specific bioremediation strategies in similar mining-impacted environments worldwide.

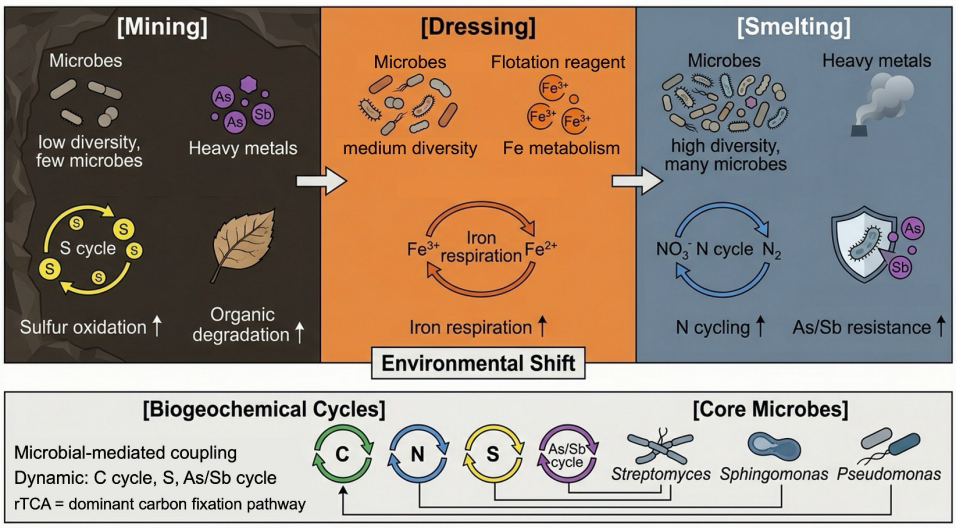


## 1. Introduction

Antimony (Sb) is a metalloid naturally found in the Earth's crust, with soil concentrations averaging between 0.2 and 0.3 mg/kg [1]. Anthropogenic activities, such as mining, smelting, and fossil fuel combustion, significantly contribute to the influx of Sb into ecosystems [2]. Mining areas and their surrounding regions generally contain elevated concentrations of Sb, with reported values ranging from 100 to 5054 mg/kg, far exceeding background levels [3]. Sb levels in nearby agricultural soils have also been reported to exceed the maximum permissible concentration recommended by the World Health Organization (WHO) [4]. Sb contamination can severely affect water quality, aquatic organisms, and food safety, posing long-term risks to both ecosystems and human health [5,6]. Therefore, controlling Sb-related environmental risks has become a critical issue in mining-impacted areas [7].

The biogeochemical cycling of Sb is largely mediated by microorganisms capable of Sb transformation, which regulate its toxicity, mobility, and bioavailability [8,9]. Microbial oxidation of Sb is particularly important as it converts the more toxic Sb(III) into the less toxic Sb(V) [10]. Previous studies have demonstrated that microbial communities in metalloid-contaminated environments are highly responsive to environmental variations associated with mining activities [11,12]. In Sb mining regions, however, such environmental variations are not generated by a single disturbance, but by a sequence of mineral processing activities including mining, dressing, and smelting.

Mining activities typically lead to soil structure destruction, vegetation loss, and the accumulation of waste materials, resulting in nutrient depletion and heavy metal contamination [11,13]. Dressing processes involve crushing, grinding, and flotation, during which flotation reagents such as xanthates can interact with heavy metals and alter their environmental behavior [14]. These reagents may also exert strong selective effects on soil microbial community diversity and structure [15]. Smelting processes, in contrast, consume large amounts of fuel and introduce complex contaminants into soils, thereby altering nutrient inputs and environmental conditions [16,17]. In addition, long-term heavy metal contamination in mining areas has been shown to generate strong spatial heterogeneity in soil microbial communities [18].

Taken together, these findings indicate that mining, dressing, and smelting are not only sources of contamination, but also drivers of heterogeneous environmental conditions, including differences in pollutant characteristics, nutrient status, and substrate availability. Such differences are likely to impose distinct selective pressures on soil microbial communities, thereby influencing their assembly and functional potential.

In heavy metal-contaminated and oligotrophic environments, metal-tolerant microorganisms can develop adaptive metabolic strategies that contribute to nutrient cycling [19–21]. For example, Serratia spp. have been shown to couple arsenite oxidation with nitrogen and carbon fixation in mine tailings [22], and phosphate-solubilizing microorganisms can significantly increase available phosphorus in contaminated soils [23]. Furthermore, co-contamination of As and Sb has been reported to reshape microbial community structure and functional pathways related to carbon, nitrogen, and sulfur cycling [13].

However, previous studies have mainly focused on individual mining-related environments, such as mining or smelting sites, or on specific aspects of microbial responses under Sb/As contamination [8,12,16]. As a result, the functional differentiation of microbial communities across sequential mining, dressing, and

 https://doi.org/10.53941/ges.2026.100013

smelting stages remains insufficiently understood. Therefore, the core scientific question of this study is how sequential mineral processing activities generate distinct environmental pressures that drive the taxonomic and functional differentiation of soil microbial communities. To address this question, a typical abandoned Sb mine was selected to investigate (i) the geochemical differences among mining, dressing, and smelting areas; and (ii) the corresponding shifts in microbial community composition and functional potential, with particular emphasis on C, N, S, and As/Sb cycling. The outcomes of this study can provide a comparative framework for understanding microbial adaptation to different mineral processing stages, help identify microbial indicators and functional traits associated with metalloid-contaminated soils, and offer a theoretical basis for future studies and site-specific bioremediation strategies in similar mining-impacted environments.

## 2. Materials and Methods

### *2.1. Sample Collection*

Soil samples in this study were collected in 2023 from mining, dressing and smelting areas in an abandoned antimony mining site located in Dafu Town, Anhua County, Yiyang City, Hunan Province, China. The sampling was conducted under sunny weather conditions. Due to long-term mining activity, these sites presented high concentrations of Sb and As. The studied antimony mining area has been abandoned for more than a decade, based on field investigation and local information. A total of three sampling plots (10 m × 10 m) were established in each area (mining, dressing and smelting). Within each plot, five sub-samples were collected and homogenized to form one composite sample.

The sampling sites in the mining area were located in proximity to mine adits and ore deposits. The dressing site occupied an area of approximately 2000 $m^2$, where dressing waste was stored in open-air piles. In the mineral dressing process, flotation reagents such as xanthates are commonly used. These sulfur-containing compounds can interact with metal ions and influence their environmental behavior. Residual flotation reagents may persist in tailings and surrounding soils, potentially affecting microbial metabolic processes, particularly those related to redox reactions. The smelting facility was located near a river, with a settling pond for smelting waste positioned on the riverbed, indicating potential inputs from smelting residues and wastewater.

The soil samples (~0–20 cm depth) in the three areas were collected according to a random sampling procedure respectively. After collection, a portion of each soil sample was immediately preserved with dry ice for transportation to the laboratory with three replicates before DNA extraction. The remaining portion of each sample was transported at ambient temperature and air-dried for the determination of soil physicochemical properties with six replicates.

### *2.2 Analysis of Physicochemical Parameters*

Soil samples were air-dried naturally and subsequently ground to pass through a 100-mesh screen. The soil pH was determined using a pH meter (LEICI PHS-3C, Shanghai, China) with distilled water (g/v, 1:2.5). Total organic carbon (TOC) was quantified with the potassium dichromate oxidation spectrophotometric method [24]. The dissolved organic carbon (DOC) was extracted with distilled water (g/v, 1:2.5) and measured using a total organic carbon analyzer (TOC-L, Shimadzu, Kyoto, Japan) [25]. Total phosphorus (TP) content was measured using the alkali fusion-molybdenum antimony anti-spectrophotometric method. Total nitrogen (TN) were respectively determined through an modified Kjeldahl method, ammonium nitrogen ($NH_4^+$-N) and nitrate nitrogen ($NO_3^-$-N) concentration were determined by extraction with potassium chloride solution-spectrophotometric methods [26]. The metal(loid)s contents were measured with an inductively coupled plasma mass spectrometer (ICP-MS7800, Agilent Technologies Inc., Santa Clara, CA, USA) after fully digestion with a mixture of $HNO_3$/$HClO_4$/HF (10/4/4, *v*/*v*/*v*) using a microwave digestion system (MARS 6, CEM, Matthews, NC, USA) [8]. Quality control was ensured using certified reference materials (GBW07405) with recovery rates ranging from 92% to 105%.

### *2.3 Metagenome Sequencing and Analysis*

Total microbial DNA in soil was extracted using a FastDNA Spin Kit (MP Biomedicals, Solon, OH, USA) according to manufacturer's protocol. The DNA purity and yield were determined using a NanoDrop 2000 spectrophotometer (Thermo Scientific, Waltham, MA, USA). Metagenomic DNA libraries of each sample were constructed using the TruSeq DNA PCR-Free Library Preparation Kit (Illumina, San Diego, CA, USA) and sequenced on HiSeq 4000 platform with PE150 mode in Majorbio Bio-Pharm Technology Co. Ltd. (Shanghai, China). Functional gene abundances were normalized as reads per kilobase of gene length per million mapped reads (RPKM), which accounts for both gene length and sequencing depth and therefore allows comparison across samples. To further ensure the robustness of cross-sample comparisons, the normalized abundances of target functional genes and pathways were used in downstream statistical analyses. About 56.9 Gb raw sequence data was generated from 9 metagenomes (three replications for each sites). To obtain clean raws, duplicates, reads with >10 "N" bases, and low-quality reads (quality score ≤ 38) were removed using Trimmomatic 0.36, subsequently the clean sequences from each sample were assembled into scaffolds using

MEGAHIT v1.2.9. Scaffolds longer than 500 bp were carried for downstream analysis. Gene prediction was performed using MetaGeneMark (version 3.25). The protein coding genes in each assembled contigs were predicted using MetaGene tool, with predicted protein coding genes longer than 300 bp being retained. The non-redundant catalogs of functional genes were generated with CD-HIT (version 4.8.1) under the criteria of identity threshold of 95% and overlap threshold of 90%. the non-redundant catalog of functional genes were mapped to clean reads using BBMap, the whole abundance of gene catalog was normalized to 100%, and their relative abundance was calculated by the ratio of corresponding coverage to the total coverage. Protein-coding sequences involved in C, N, S, and As/Sb cycling were annotated using DIAMOND blastp (version 0.8.35) against the Kyoto Encyclopedia of Genes and Genomes (KEGG, Release 106.0, April 2023), eggNOG (version 5.0), and Gene Ontology (GO, release 2023-01-01) databases, with an e-value cutoff of $1 \times 10^{-5}$. The taxonomic assignment of the functional genes was conducted using MEGAN with the Last Common Ancestor method [27].

Functional genes involved in C, N, S, and As/Sb cycling were selected based on their roles in key metabolic pathways. Gene annotation was performed using the KEGG database, and genes representing core enzymatic steps in each element cycling process were identified according to established pathway frameworks. Only genes detected in the metagenomic dataset were included in subsequent analyses to ensure ecological relevance.

### *2.4. Statistical Analyses*

All statistical analyses and visualization were conducted through SPSS 21.0 or the R 4.2.1 software The comparison of geochemical parameters across three site was performed using one-way ANOVA by using SPSS 21.0. Differences in normalized functional gene abundances among mining, dressing, and smelting areas were also evaluated using one-way ANOVA based on RPKM-normalized values. Principal coordinate analysis (PCoA) based on Bray-Curtis distance and pairwise Adonis analysis were conducted using 'vegan' package in R.

## 3. Results

### *3.1. Environmental Parameters and Heavy Metal Concentrations in Mining, Dressing and Smelting Areas*

Environmental parameters and heavy metal concentrations were measured in each field (Figure 1). The average pH in mining, dressing and smelting areas was 8.52, 8.45 and 8.45. The nutrient elements, mainly TOC, TP and TN were higher in mining soils than those of smelting, with the values being 14.5 g/kg, 1358 mg/kg and 3028 mg/kg respectively in mining areas ($p < 0.05$), and no significant difference among three regions was observed in $NH_4^+$-N and $NO_3^-$-N. In addition, Except of Cu, the As, Sb, Zn, Fe, and Mn concentrations in the three sites did not show significant differences ($p > 0.05$).

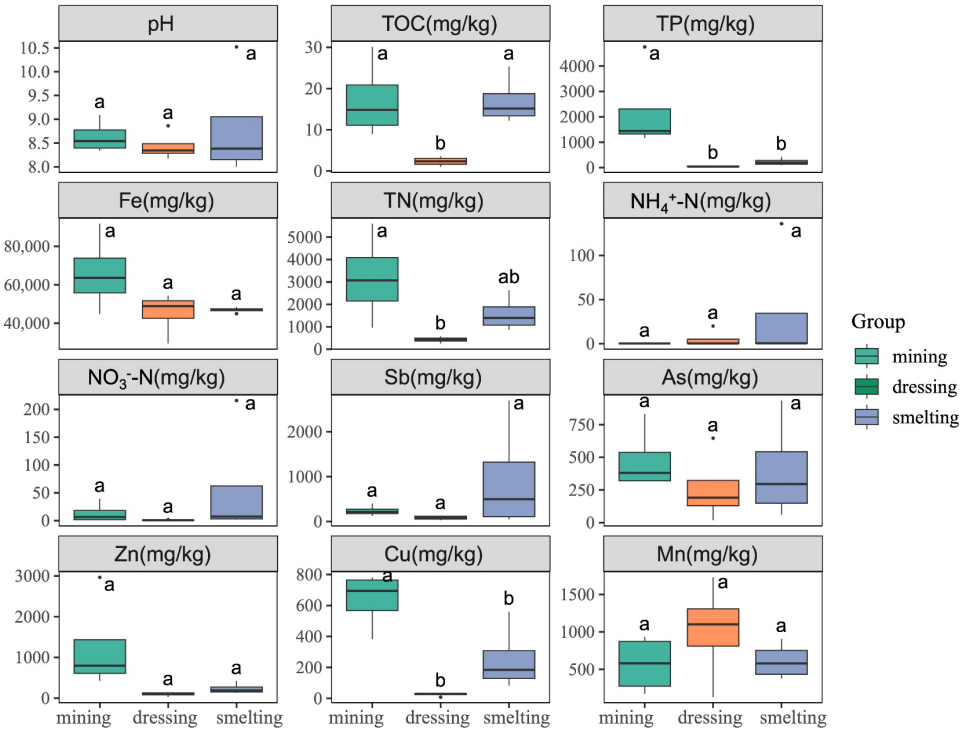


**Figure 1.** Boxplot showing the distribution of the measured concentrations of the different geochemical parameters. The different letters (a and b) above the box are significantly different ($p < 0.05$, least significant difference (LSD) test). The different colours represent the different sample regions.

 https://doi.org/10.53941/ges.2026.100013

### *3.2 Microbial Communities Influenced by Mining, Dressing and Smelting Activities*

Analysis of α- and β-diversity revealed distinct patterns across the three sites. For α-diversity (Figure 2A), diversity indices differed significantly among the study areas. The dressing area supported bacterial communities with moderate diversity, characterized by mean Shannon, Simpson, ACE, and Chao indices of 5.56, 0.02, 2213.47, and 2116.12, respectively. The mining area exhibited the lowest bacterial diversity: its mean Shannon (5.14), ACE (1101.40), and Chao (1136.79) indices were lower than those in the other two areas, while the Simpson index (0.02) was comparable to that of the dressing area. In contrast, the smelting area harbored the most diverse bacterial communities, with the highest mean values across all indices (Shannon: 6.35; Simpson: 0.06; ACE: 2760.92; Chao: 2733.31). These observations suggest that mining activities exerted the strongest inhibitory effect on soil bacterial richness and diversity, whereas the smelting area sustained relatively greater bacterial community diversity and species richness.

For β-diversity (Figure 2B), PCoA indicated that the first two principal coordinates (PC1 and PC2) accounted for 32.06% and 19.69% of the total variation in community composition, respectively. Samples from each site formed distinct clusters in the ordination space: those from the mining area clustered independently, while samples from the dressing and smelting areas showed partial overlap but remained distinguishable. These results demonstrate that mining, dressing, and smelting activities drive distinct shifts in soil bacterial community composition, consistent with the differentiation trends observed in α-diversity.

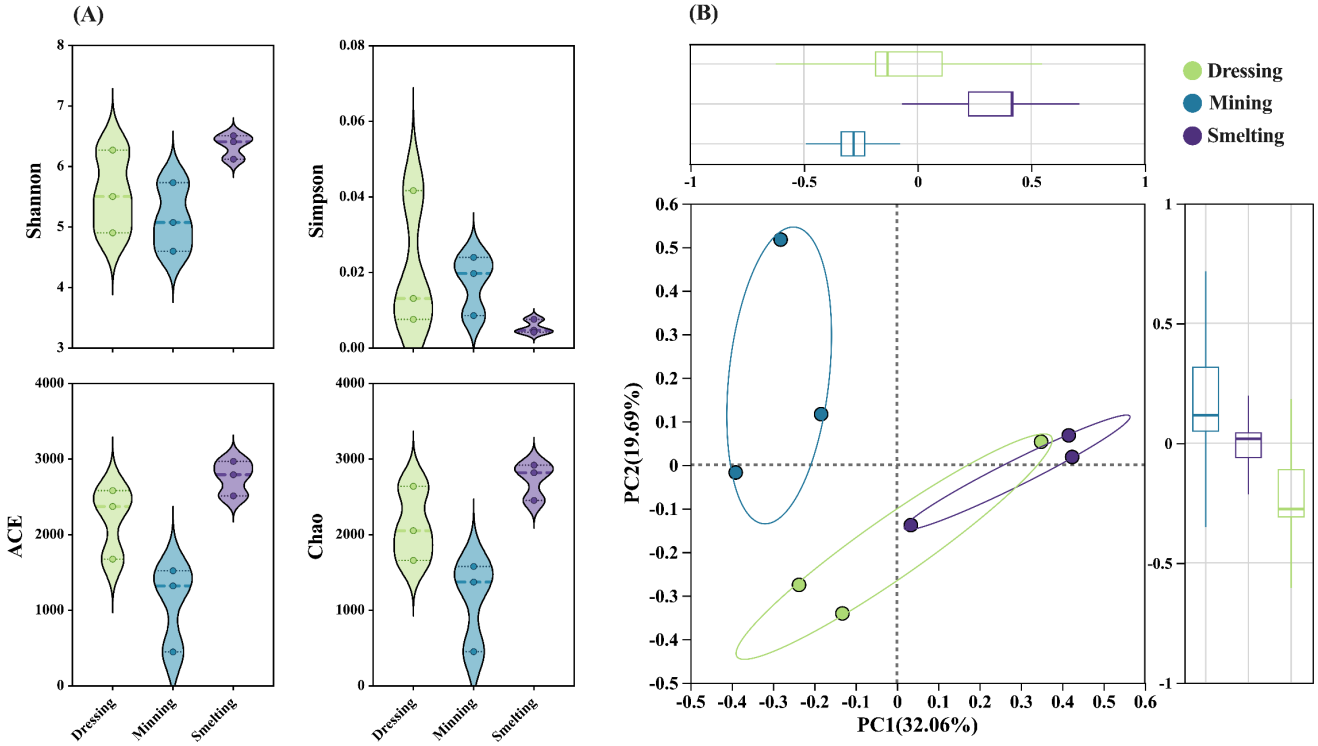


**Figure 2.** Soil microbial α- and β-diversity at the three sampling regions. (**A**) α-diversity indices (Shannon, Simpson, ACE, and Chao); (**B**) β-diversity based on principal coordinate analysis (PCoA).

The Kraken 2 was used to identify the microbial community composition based on reads information (Figure 3A,B). The *Proteobacteria, Acidobacteria, Chloroflexi* and *Actinobacteria* were the most abundant phylum in mining, dressing and smelting areas, with their relative abundance being 8.73–48.32%, 2.36–22.89%, 1.55–18.35% and 2.79–14.25% respectively, and the archaea was mainly affiliated to *Thaumarchaeota* and *Euryarchaeota*. The mineral utilization activities potential affected the microbial community composition at phylum level, and mining activities were associated with higher relative abundances of *Proteobacteria* and *Firmicutes*. *Actinobacteriota* also showed a relatively higher proportion in the mining group compared to the other treatments, while decreased *Acidobacteria, Chloroflexi* and *Thaumarchaeota.* The main genus in the three sites was *Microcella, Nitrosotalea, Pseudomonas, Bacillus, Limnobacter* and *Bradyrhizobium*, and their relative abundance was 0.01–7.85%, 0.01–0.84%, 0.12–1.42%, 0.01–2.51%, 0.01–2.38%, and 0.24–0.96%. Mining activities were associated with higher relative abundances of *Microcella* and *Bacillus* compared to the other treatments. In contrast, *Anaeromyxobacter* showed the highest relative abundance in the dressing area.

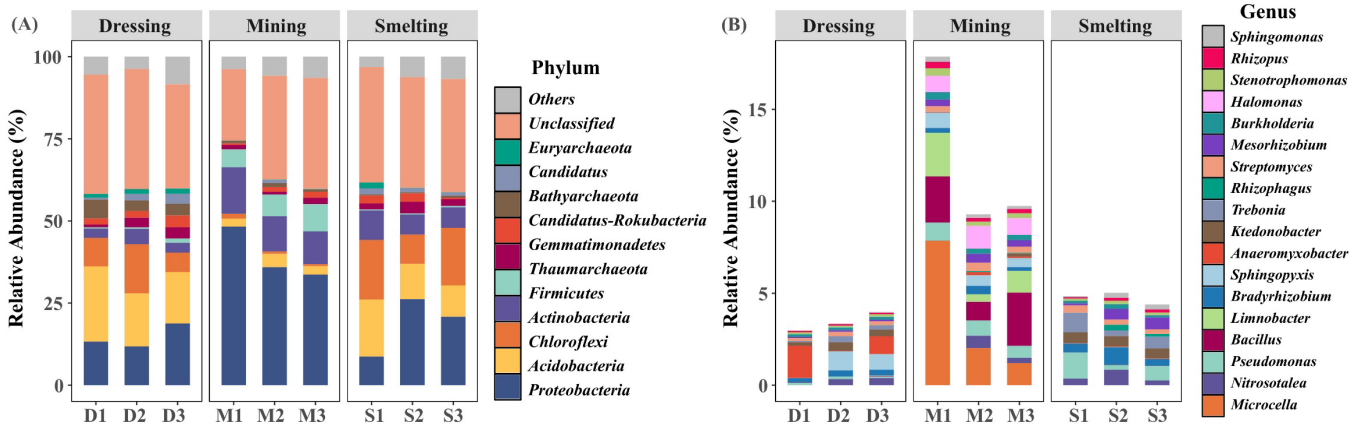


**Figure 3.** Soil microbial community composition at the three sampling regions, showing the 12 most abundant phylum (**A**) and the 18 most abundant genus (**B**). M1–M3 represent the three replicate samples from the mining area; D1–D3 represent the three replicate samples from the dressing area; and S1–S3 represent the three replicate samples from the smelting area.

To further quantify the effects of environmental gradients on microbial community composition across the three processing-stage areas, redundancy analysis (RDA) was performed using the measured soil physicochemical variables (Figure 4A). The first two ordination axes (RDA1 and RDA2) together explained 83.08% of the total variation in community composition, indicating that environmental factors accounted for a substantial proportion of the observed microbial differentiation among samples. Monte Carlo permutation testing showed that the overall explanatory effect of the selected environmental variables was significant ($p < 0.05$), confirming that environmental heterogeneity was a major driver of microbial community variation.

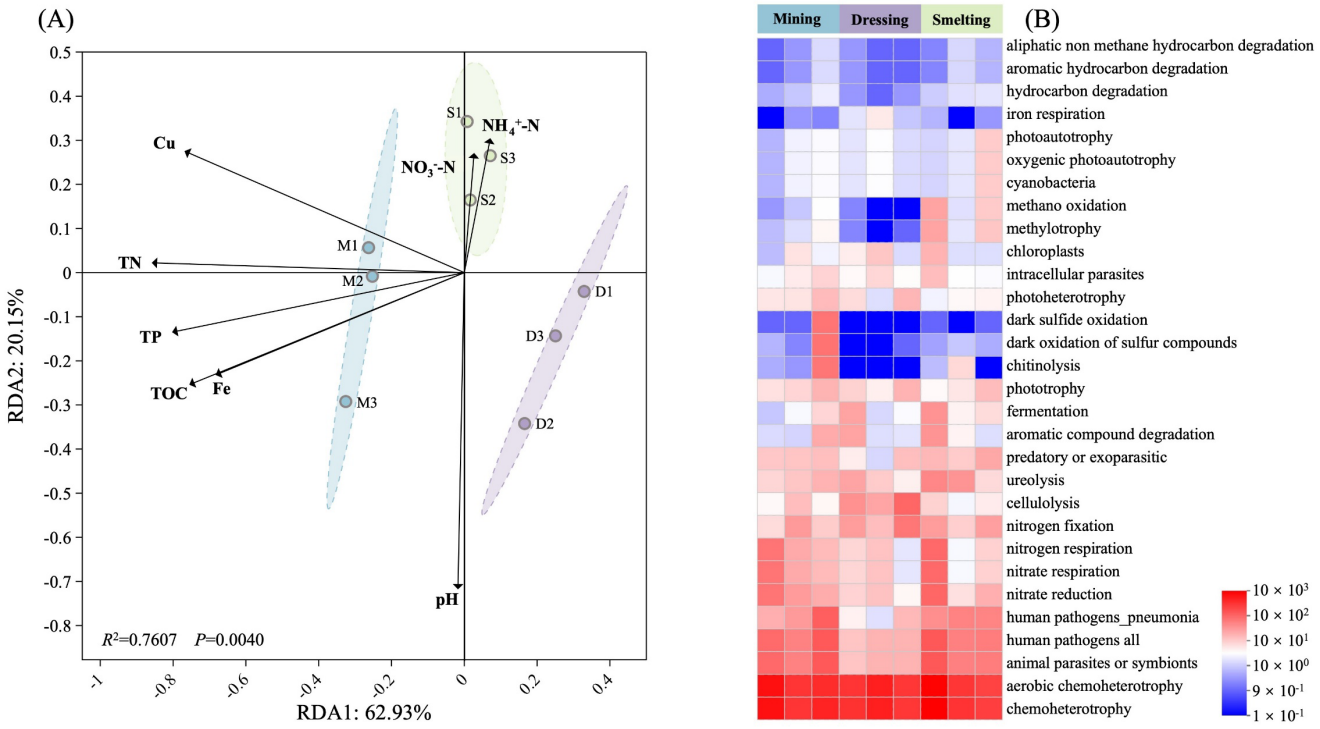


**Figure 4.** Soil redundancy analysis (**A**) and microbial functional prediction analysis (**B**).

The samples from the mining, dressing, and smelting areas were clearly separated in the RDA space, further demonstrating marked differences in microbial community composition among the three regions. Among the tested environmental variables, carbon, nitrogen, and phosphorus nutrients, pH, Cu, and Fe showed relatively strong explanatory power for the distribution of microbial taxa, suggesting that both nutrient status and geochemical stress jointly shaped community assembly. In particular, the smelting samples were positioned closer to $NH_4^+$-N and $NO_3^-$-N, indicating that nitrogen availability was more strongly associated with microbial community composition in the smelting area and that the microbial

taxa in this region may be better adapted to, or selectively favored by, N-enriched conditions.

Functional prediction analysis revealed distinct variations in the relative abundances of key metabolic functions across the three sites (Figure 4B). The high abundance of iron respiration in the dressing area is closely related to the flotation reagents used in ore dressing, which can complex with Fe ions in the soil and directly select for microbes capable of utilizing Fe as an electron acceptor. In contrast, methanol oxidation and methylotrophy functions were most abundant in the smelting area, with the lowest levels detected in the dressing area. For sulfur-related metabolic functions, including dark sulfide oxidation and dark oxidation of sulfur compounds, the mining area showed substantially higher functional abundances than the other two sites. Similarly, chitin decomposition was most enriched in the mining area, with relatively low levels in the dressing and smelting areas.

These patterns suggest that mining, dressing, and smelting activities have shaped the functional specialization of soil bacterial communities: the dressing area is enriched in iron-related respiratory functions, the smelting area favors methanol-based metabolic pathways, and the mining area supports enhanced sulfur oxidation and chitinolytic processes.

### *3.3 Metabolic Potentials Revealed by Metagenomic Analysis*

To survey the distribution of functional genes and pathways of C fixation, N, S, As cycling and metal resistance microbiomes in three sites based on based on metagenome, we analysed the relative abundance of above functional genes and their community composition.

According to Figure 5, functional genes involved in the C fixation were divided into 3-hydroxypropionate bicycle (3-HP), dicarboxylate-hydroxybutyrate cycle (DC/4-HB), hydroxypropionate-hydroxybutylate cycle (3-HP/4-HB), reductive acetyl-CoA pathway (Wood-Ljungdahl pathway), reductive pentose phosphate cycle (Calvin cycle; CBB) and the reductive citric acid cycle (Arnon-Buchanan cycle; rTCA). A higher relative abundance of genes related to rTCA (0.34–0.46%), DC/4-HB (0.20–0.28%) and 3-HP (0.18–0.22%) was observed, and dressing areas contained lower abundant of genes involved in DC/4-HB and WL pathways ($p < 0.05$). The microbial composition of C fixation genes at the taxonomic level of genera was mainly *Streptomycetales, Sphingopyxis, Sphingomonas, Pseudomonas, Nocardioides, Mycobacterium,* and so on, and the relative abundances of carbon-fixation genes and taxonomic assignments were constant among three sites. In addition, smelting area contained higher relative abundance of *Sphingomonas* and *Microcella*.

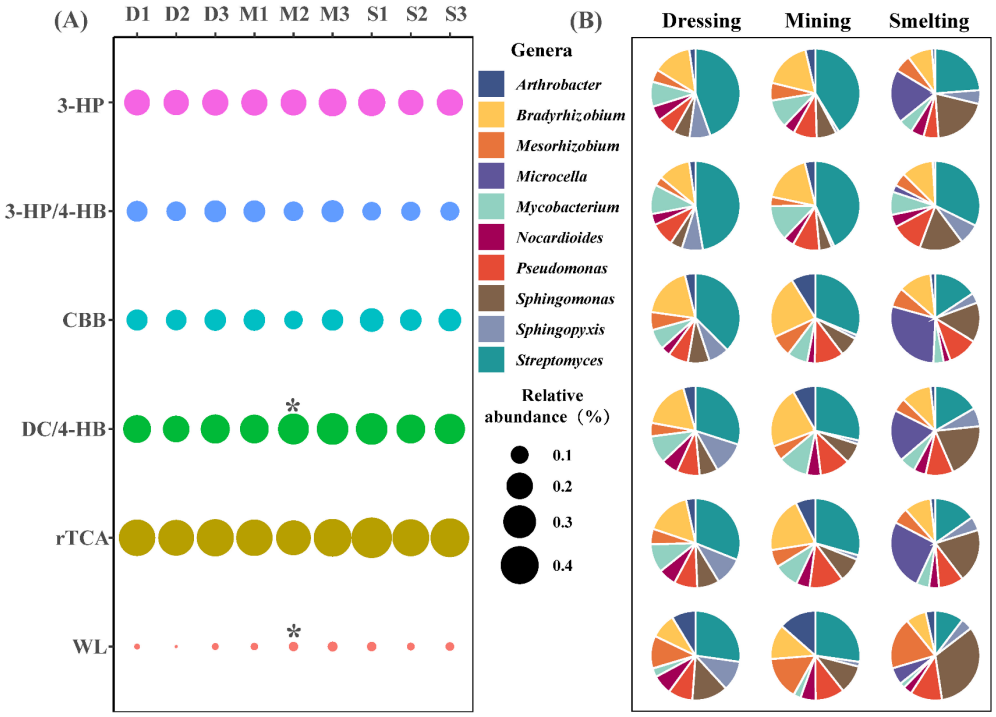


**Figure 5.** Relative abundance (**A**) and genera assignments (**B**) of genes for carbon fixation. Asterisks (*) indicate significant differences ($p < 0.05$).

All the functional genes related to the N cycling were divided into N fixation, nitrification, nitrate reduction, denitrification, anammox/hydroxylamine oxidation and N degradation (Figure 6). The sites of dressing and mining presented similar distribution of N cycling genes, while smelting sites exhibited higher relative abundance of *nir,*

*nrt, glt* and *nas,* which were affiliated to nitrate reduction and nitrate transport. The microbial composition of N cycling genes at the taxonomic level of genera was mainly *Streptomyces, Sphingomonas, Serpentinimonas, Pseudomonas, Nitrospira, Mycobacterium and Microcella.*

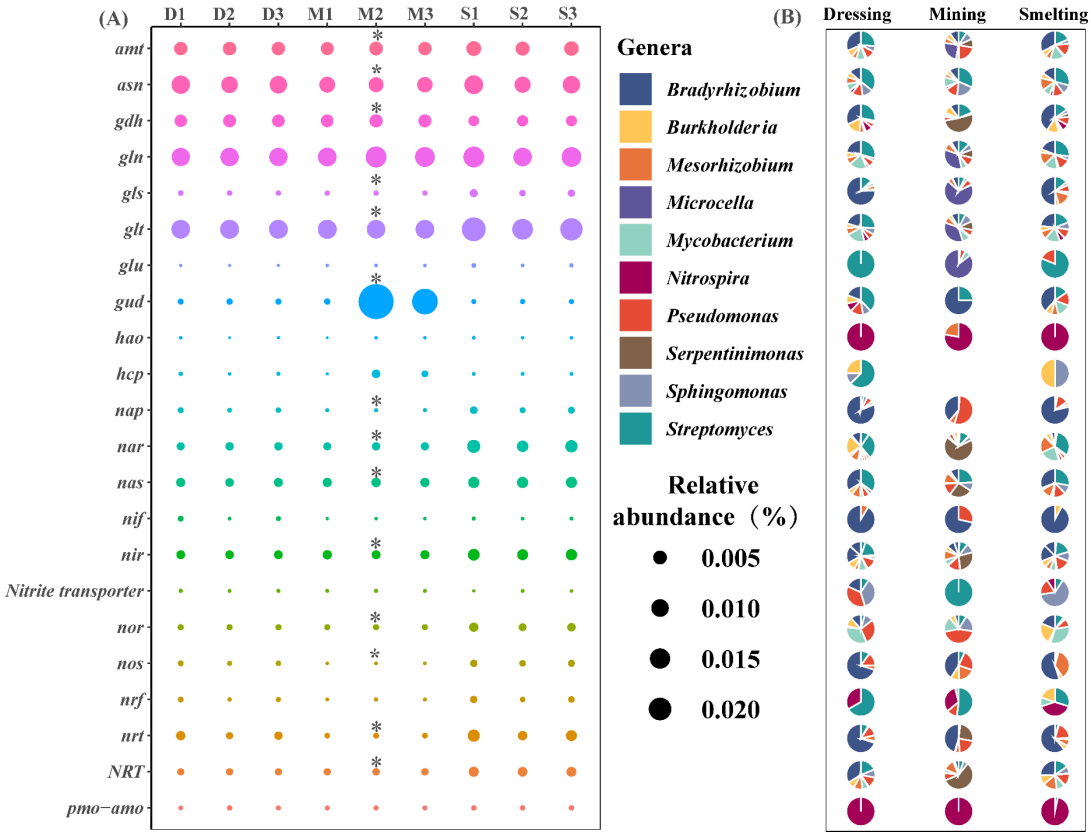


**Figure 6.** Relative abundance (**A**) and genera assignments (**B**) of genes for N cycling. Asterisks (*) indicate significant differences ($p < 0.05$).

Functional genes involved in the S cycling were divided into dissimilatory sulfate reduction, assimilatory sulfate reduction and thiosulfate oxidation (Figure 7). The sites of dressing and mining presented similar distribution of S cycling genes, while smelting sites possessed higher relative abundance of *soxABXYZ, cysIJDNC* and *aprAB,* which were affiliated to dissimilatory sulfate reduction and thiosulfate oxidation. The microbial composition of S cycling genes at the taxonomic level of genera was mainly *Thiobacillus, Thioalkalivibrio, Streptomyces, Sphingopyxis, Sphingomonas* and *Pseudomonas.*

As and Sb share similar physicochemical properties and speciation transformation processes, as both elements belong to the same group in the periodic table and commonly occur as trivalent and pentavalent species in the environment [28,29]. Therefore, the environmental behavior and biotransformation of Sb are often interpreted based on knowledge derived from As studies [30]. Functional genes involved in the As/Sb cycling were divided into oxidation, reduction, and methylation/demethylation processes (Figure 8). The sites of dressing and mining presented similar distribution of As/Sb cycling genes, and showed higher relative abundance of *aoxAB* and *ASNA1*, which were potentially involved in Sb oxidase and transport. While smelting sites possessed higher relative abundance of *ACR3, arsH and arsC,* which were affiliated to Sb reductase, transport and resistance. The microbial composition of Sb cycling genes at the taxonomic level of order was mainly *Thermoflexus, Streptomyces, Sphingopyxis, Sphingomonas* and *Pseudomonas.*

Taken together, the distribution of functional genes revealed clear stage-specific patterns across mining, dressing, and smelting areas. The mining area favored metabolic pathways related to sulfur oxidation and organic matter degradation, reflecting adaptation to sulfur-rich and nutrient-limited conditions. The dressing area was primarily associated with iron-related metabolic functions, likely influenced by flotation reagents and tailing composition. The smelting area exhibited enhanced functional potential in nitrogen transformation, sulfur cycling, and metalloid resistance, suggesting stronger selection for microbes capable of coping with complex contamination and geochemical stress. These results highlight the functional differentiation of microbial communities along the mineral processing gradient.

 https://doi.org/10.53941/ges.2026.100013

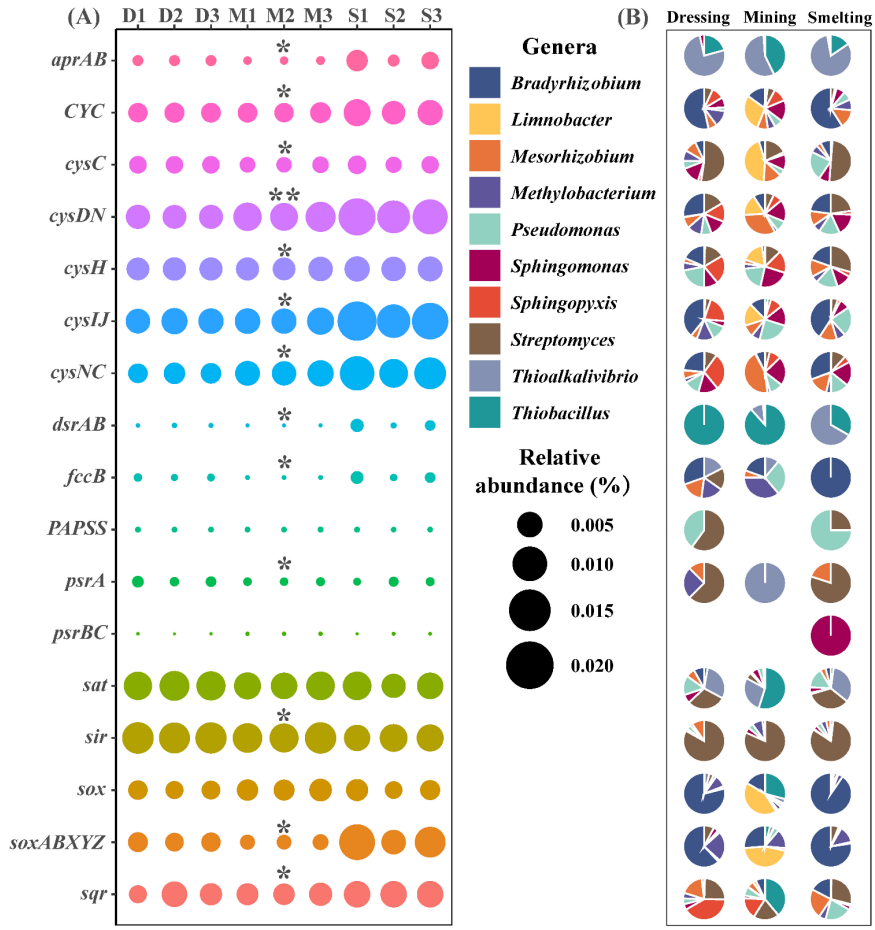


**Figure 7.** Relative abundance (**A**) and genera assignments (**B**) of genes for S cycling. Asterisks (*/**) indicate significant differences ($p < 0.05$/$p < 0.01$).

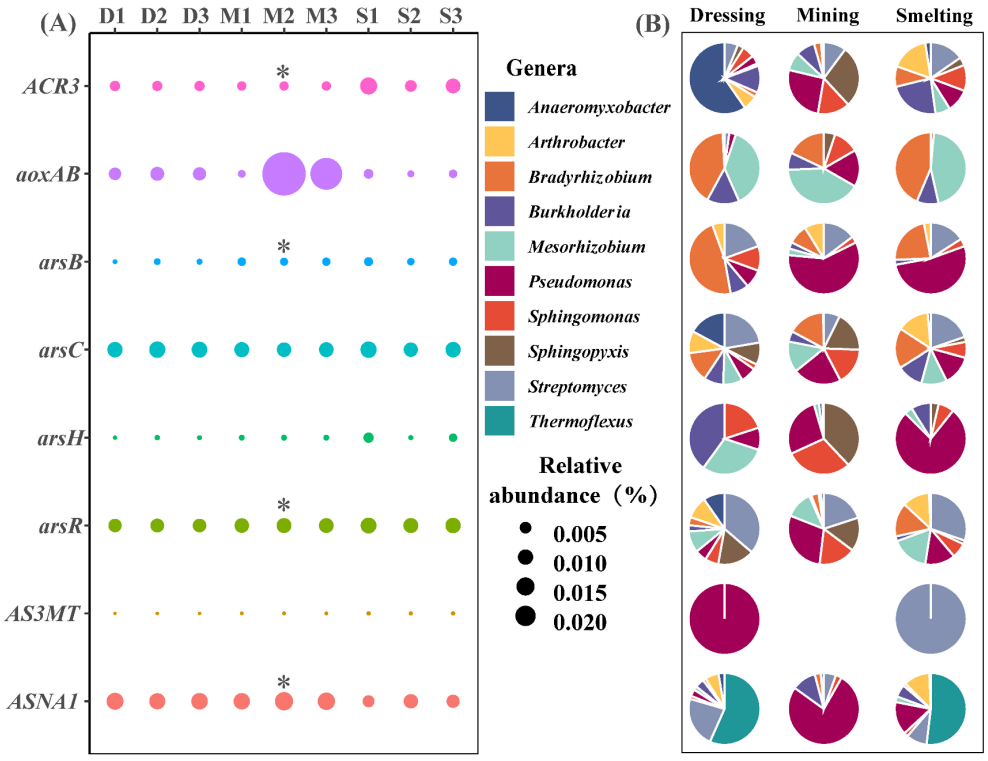


**Figure 8.** Relative abundance (**A**) and genera assignment (**B**) of functional genes involved in As cycling across the three sampling regions. Asterisks (*) indicate significant differences ($p < 0.05$).

## 4 Discussion

### *4.1 Environmental Drivers of Microbial Community Differentiation*

Soil physicochemical properties are well recognized as key determinants of microbial community structure, and this study indicates that mining, dressing, and smelting activities are closely associated with variations in microbial assemblages, potentially driven by site-specific modifications to nutrient levels and metal(loid) concentrations. Variations in nutrient availability and metal(loid) concentrations are well known to influence microbial community assembly and functional potential. Recent studies have shown that heavy metal contamination can significantly alter microbial community structure and interactions, acting as an important environmental driver in soil ecosystems [31,32]. In addition, soil physicochemical properties such as nutrient availability and environmental conditions have been reported to regulate microbial community composition and ecological functions [33,34]. This interpretation is consistent with recent evidence from Sb-contaminated soils showing that pH, nutrient availability, and metal(loid) distribution are major determinants of microbial community assembly [35]. More broadly, soil microbiomes are increasingly recognized as being structured by interacting gradients in soil chemistry, nutrient status, and hydrological conditions, rather than by isolated edaphic variables [36]. Therefore, the distinct microbial patterns observed in this study are likely linked to site-specific environmental conditions created by different mineral processing activities. This interpretation was further supported by the RDA results, in which the first two ordination axes explained 83.08% of the variation in microbial community composition and the Monte Carlo permutation test indicated a significant overall effect of the measured environmental variables ($p < 0.05$). These results confirm that microbial differentiation across the mining, dressing, and smelting areas was jointly driven by multiple environmental gradients rather than by a single factor.

Our results showed that Sb, As, Zn, and Mn exhibited consistent distribution across the three sites, reflecting the unified pollution source from mineral processing including metalloid-laden refuse ore, dust, and wastewater as reported by Liang et al. [23]. This consistency is further reinforced by the coexistence and concurrent release of As and Sb, which is attributed to their similar physicochemical properties according to Okkenhaug et al. [37]. In contrast, nutrient elements (TOC, TN, TP) and Cu concentrations varied significantly among sites. The mining area exhibited higher TOC, TN, and TP concentrations than the dressing and smelting areas. This pattern may be attributed to differences in the types of disturbance and material inputs associated with each processing stage, rather than disturbance intensity alone. In mining areas, exposed ores and waste rocks are often accompanied by residual organic matter and partial vegetation recovery after site abandonment, which can contribute to the accumulation of soil nutrients over time. In contrast, dressing areas are typically dominated by tailings and flotation residues, which are generally poor in organic matter and nutrients, leading to reduced TOC and TN levels. Similarly, smelting activities involve high-temperature processing and the release of metal-rich wastes, which can disrupt soil structure and accelerate the decomposition or loss of organic matter. Previous studies have also reported that different mineral processing stages create distinct geochemical environments, resulting in contrasting nutrient dynamics and microbial responses [13,21]. Therefore, the observed nutrient differences among sites are more likely driven by differences in material composition and biogeochemical processes associated with mining, dressing, and smelting, rather than disturbance intensity alone.

These environmental gradients directly drove differences in microbial diversity. The mining area maintained relatively constrained nutrient availability compared to the other two sites, a pattern linked to soil structure disruption and nutrient leaching from long-term ore extraction as noted by Li et al. [13]. When combined with high Sb/As concentrations, this nutrient limitation explains the lowest bacterial α-diversity observed in the mining area. This aligns with previous reports that nutrient scarcity and heavy metal stress synergistically suppress microbial richness and diversity [21]. It also extends these findings by showing that even moderate nutrient retention relative to other processing sites cannot offset the toxic effects of high metalloid concentrations. In contrast, the smelting area supported the highest bacterial diversity. In addition to smelting-derived organic inputs, such as fuel combustion residues that may provide additional carbon sources [17], the environmental setting of the smelting area may also have contributed to microbial diversity. The smelting facility was located near a river, with a settling pond positioned on the riverbed, suggesting potential differences in hydrological conditions, including soil moisture, aeration status, and redox environment, compared with the mining and dressing areas. These factors influence microbial community assembly and diversity. Therefore, the relatively high diversity observed in the smelting area was more likely shaped by the combined effects of nutrient availability, hydrological conditions, and local geochemical characteristics.

These site-specific environmental gradients are the core drivers of distinct microbial community composition. The RDA ordination showed clear separation among samples from the mining, dressing, and smelting areas, further confirming that the three processing-stage environments supported significantly differentiated microbial assemblages. Mining-disturbed soils typically select for taxa adapted to high heavy metal(loid)

 https://doi.org/10.53941/ges.2026.100013

concentrations and fluctuating nutrient levels [38]. Our study identified dominant phyla including *Proteobacteria*, *Acidobacteria*, *Chloroflexi*, *Actinobacteria* and genera such as *Pseudomonas*, *Bradyrhizobium*, *Sphingopyxis* that are consistent with those reported in other mining areas [21]. It advances understanding by linking their enrichment to the unique environmental conditions of each processing stage. For example, *Proteobacteria* and *Actinobacteria* were enriched in the mining area. Genera such as *Pseudomonas* and *Bacillus* possess specific functional traits that enable survival under high metalloid stress. Similarly, *Sphingopyxis* enriched in the smelting area correlates with the high Sb concentration and functional specialization of the smelting site.

The PCoA results showed that the mining area microbial community clustered independently, while the dressing and smelting communities exhibited partial overlap. This distinct clustering reflects the strong and unique selective pressure of mining-induced environmental stress [18]. Our study further clarifies that this pressure is mediated by the combined effects of nutrient status, pH, and metal(loid)-related geochemical conditions, rather than by any single environmental factor. This interpretation is directly supported by the RDA results, which identified C, N, P, pH, Cu, and Fe as the major variables associated with community differentiation across the three processing stages. The partial overlap between dressing and smelting communities suggests that their environmental conditions such as similar nutrient levels and distinct functional pollutant inputs select for overlapping but specialized taxa. This nuance is rarely captured in studies comparing only two processing stages.

### *4.2 Adaptive Traits of Dominant Microbial Taxa and Functional Specialization*

*Proteobacteria*, *Actinobacteria*, and *Firmicutes* were enriched in the mining area, with *Pseudomonas*, *Bacillus*, and *Bradyrhizobium* as the dominant genera. This aligns with the well-documented tolerance of these taxa to heavy metals and nutrient-poor conditions [39,40]. For example, *Bacillus* species possess cell wall peptidoglycan layers with active adsorption sites such as teichoic acid that facilitate heavy metal sequestration [39], while *Pseudomonas* employs multiple mechanisms including reduction and volatilization to mitigate metal toxicity [41]. *Bradyrhizobium*, a core taxon in As/Sb-contaminated soils, may contribute to nitrogen cycling in the nutrient-limited mining area via nitrogen fixation and denitrification [42]. This highlights the functional trade-offs of microbial communities in stressed environments, where taxa must balance metal tolerance with nutrient acquisition to persist.

The functional prediction results showed that the dressing area had a significantly higher abundance of iron-related respiratory functions compared with the mining and smelting areas. In light of the RDA results, this pattern is more appropriately interpreted as being jointly associated with Fe and Cu geochemistry, nutrient conditions, and possible flotation-reagent residues. These compounds may interact with Fe and other metal ions, thereby contributing to local redox conditions that favor microbes capable of Fe-associated respiratory metabolism [15]. The smelting area showed higher methanol oxidation and methylotrophy functions than the other two sites, with the dressing area having the lowest values. This likely reflects the availability of smelting-derived methylated compounds such as methanol as carbon sources [16], consistent with the role of *Sphingomonas* (a dominant genus in the smelting area) in methyl compound metabolism [43]. The mining area exhibited higher abundances of dark sulfide oxidation, dark oxidation of sulfur compounds, and chitinolysis compared to the dressing and smelting areas. This suggests adaptations to sulfur-rich ore residues and chitin-containing organic debris such as plant residues. Sulfur-oxidizing microbes including *Thiobacillus* and chitinolytic taxa such as *Streptomyces* are known to thrive in such habitats [27,44], and their enrichment underscores how mining-induced substrate availability shapes functional specialization.

Our study identified consistent patterns in core biogeochemical cycling pathways across sites, while also highlighting taxon-specific contributions to these processes. This interpretation is also consistent with the RDA results, in which the smelting samples were positioned closer to $NH_4^+$-N and $NO_3^-$-N. Together, these findings suggest that nitrogen availability was an important ecological filter in the smelting area and likely contributed to the enrichment of nitrate transformation potential in this site. Among six carbon fixation pathways evaluated, little variation was observed across sites, with the reductive citric acid cycle (rTCA) showing the highest relative abundance and the Wood-Ljungdahl pathway the lowest. This pattern mirrors findings in acid mine drainage-impacted soils and may reflect the prevalence of chemoautotrophic microbes in metalloid-contaminated environments [45]. Heavy metal(loid)s are known to induce the expression of carbon fixation-specific enzymes in taxa such as *Thiomonas arsenivorans* [45], and the high As/Sb concentrations in our study sites likely select for such chemoautotrophs to maintain carbon cycling functionality. For nitrogen cycling, genes encoding nitrite reductase accounted for a large proportion of total nitrogen cycling genes, indicating active denitrification. This process may help microbial communities cope with nutrient limitation by recycling nitrogen compounds. Under the aerobic conditions observed in our study soils, functional genes involved in assimilatory sulfate reduction and thiosulfate oxidation were more abundant than those linked to dissimilatory sulfate reduction [27], reflecting

adaptive metabolic strategies to utilize sulfur sources efficiently in oxygen-rich, metalloid-stressed environments.

Our study identified *Streptomyces*, *Sphingopyxis*, *Sphingomonas*, and *Pseudomonas* as universal genera involved in C, N, S, and As/Sb cycling across all three sites. This extends previous research by demonstrating that these taxa are not only tolerant to metalloid stress but also serve as keystone players in integrating multiple biogeochemical cycles in contaminated soils. For example, *Streptomyces* and *Sphingopyxis* (enriched in the smelting area) are associated with Sb resistance and oxidation [43], while also contributing to sulfur oxidation and carbon fixation. *Sphingopyxis* has been specifically linked to Sb transport gene (*arsB*) upregulation under Sb pollution [43], further supporting its role in metalloid cycling. Their versatility makes them promising candidates for bioremediation, as they can simultaneously mitigate metalloid toxicity and enhance nutrient cycling to support ecosystem recovery.

The functional specialization of each site such as sulfur oxidation in mining areas and iron respiration in dressing areas suggests that site-specific bioremediation strategies may enhance efficiency. By targeting the keystone taxa and their associated metabolic pathways identified in this study, remediation efforts can leverage the inherent adaptive traits of microbial communities rather than relying on exogenous microbes with uncertain survival potential. For practical bioremediation, sulfur-oxidizing microbes (e.g., *Thiobacillus*) could be augmented in mining areas to enhance the biotransformation of toxic Sb(III) to less toxic Sb(V), while iron-respiring taxa could be harnessed in dressing areas to facilitate the degradation of residual flotation reagents.

Collectively, mining, dressing, and smelting activities drive distinct shifts in soil microbial diversity, composition, and function through modifications to nutrient levels and metal(loid) concentrations. Dominant microbial taxa have evolved site-specific adaptive traits to cope with environmental stressors, while simultaneously mediating critical biogeochemical cycles. These findings provide a theoretical basis for microbial-based remediation strategies.

### *4.3 Practical Implications for Bioremediation and Environmental Restoration*

The present study provides a comparative framework for linking mineral processing stages with microbial community assembly and functional differentiation in Sb-contaminated soils. These findings have practical implications for environmental restoration in mining-impacted areas.

First, the clear differences in microbial community composition and metabolic potential among mining, dressing, and smelting areas suggest that bioremediation strategies should be site-specific rather than uniform across the entire mining system. For example, the mining area was characterized by stronger sulfur oxidation potential and enrichment of metal-tolerant taxa, indicating that sulfur-oxidizing and metalloid-resistant microorganisms may play important roles in promoting Sb transformation and ecological recovery in mine-disturbed soils. In the dressing area, the relatively high abundance of iron-related respiratory functions suggests that microbial processes associated with iron transformation may be particularly relevant for the stabilization or degradation of flotation-related residues. In the smelting area, where genes related to nitrate transformation, sulfur metabolism, and As/Sb resistance were more abundant, restoration strategies may benefit from considering both metalloid detoxification and nutrient turnover processes under hydrologically influenced conditions.

Second, the identification of core taxa such as *Streptomyces*, *Sphingopyxis*, *Sphingomonas*, and *Pseudomonas* provides potential microbial indicators for monitoring ecological status and evaluating restoration effectiveness in metalloid-contaminated soils. These taxa may also serve as candidate functional groups for future hypothesis-driven studies on microbial remediation. However, their relative contributions to individual pathways were not quantitatively partitioned in the present study. Therefore, their roles are more appropriately interpreted as potential multifunctional involvement rather than confirmed functional synergy. Future analyses integrating taxon-specific functional gene contributions will help distinguish functional redundancy from specialization across mineral processing stages.

Finally, the present dataset can support future studies aimed at integrating microbial ecology with restoration design, including targeted isolation of key functional microbes, validation of critical functional genes, and testing of site-adapted remediation consortia. Therefore, beyond describing microbial patterns, this study offers a theoretical basis for developing stage-specific and microbially informed restoration strategies in abandoned antimony mining areas and similar metalloid-contaminated environments.

## 5 Conclusions

This study systematically explored the effects of mining, dressing, and smelting activities on soil physicochemical properties, microbial communities, and C, N, S, As/Sb biogeochemical cycling in an abandoned Sb mine area. These anthropogenic activities significantly altered soil nutrient (TOC, TN, TP) and copper concentrations, while all sites showed high As/Sb co-contamination with consistent As, Sb, Zn, and Mn distributions. Notable differences in microbial diversity were observed among the three sites. The mining area had the lowest bacterial α-diversity, while the smelting area

 https://doi.org/10.53941/ges.2026.100013

maintained the highest. PCoA confirmed distinct microbial community compositions, with mining activities enriching metal-tolerant taxa such as *Proteobacteria*, *Actinobacteria* and *Bacillus*, and *Bradyrhizobium*. Microbial communities showed clear functional specialization corresponding to each site's environmental characteristics. The dressing area had high iron respiration abundance, the smelting area showed elevated methanol oxidation and methylotrophy, and the mining area had enhanced sulfur oxidation and chitinolysis functions. Smelting activities increased the relative abundance of genes related to nitrate reduction, sulfate reduction, and As/Sb resistance. Key genera including *Streptomyces*, *Sphingopyxis*, *Sphingomonas*, and *Pseudomonas* were core drivers of biogeochemical cycling across sites. These findings highlight the role of mining-related activities in shaping microbial communities and provide fundamental insights for site-specific bioremediation of metalloid-contaminated soils.

## Author Contributions

W.P.: Conceptualization, methodology, software, investigation, writing—original draft, and writing—review & editing; Y.H. and W.L.: Conceptualization, funding acquisition, investigation, and writing—review & editing. B.Z.: Methodology, investigation, and writing; C.W.: Methodology, investigation, and writing—review & editing; X.X.: Conceptualization, methodology, investigation. Y.W.: Conceptualization and methodology. T.P.K.: conceptualization and methodology. All authors have read and agreed to the published version of the manuscript.

## Funding

This work is funded by the National Natural Science Foundation of China (No. 42177392), the Hunan Natural Science Fund for Distinguished Young Scholar, China (2023JJ10063), Dean's Research Fund (IRS-4 2023) from Education University of Hong Kong and Croucher Foundation, the Hunan Natural Science Fund for Distinguished Young Scholar, China (2023JJ10063), the Central South University Graduate School-Enterprise Joint Innovation Project, China (2024XQLH011).

## Institutional Review Board Statement

Not applicable.

## Informed Consent Statement

Not applicable.

## Data Availability Statement

The data of this paper are available upon request (contact yyhuang@csu.edu.cn).

## Conflicts of Interest

The authors declare no conflict of interest.

## Use of AI and AI-assisted Technologies

During the preparation of this work, the authors used ChatGPT to language polishing, sentence refinement and academic expression improvement of the manuscript. After using this tool, the authors reviewed and edited the content as needed and take full responsibility for the content of the published article.

## References

1. He, M.; Wang, N.; Long, X.; et al. Antimony Speciation in the Environment: Recent Advances in Understanding the Biogeochemical Processes and Ecological Effects. *J. Environ. Sci.* **2019**, *75*, 14–39.
2. Zhu, Y.; Yang, J.; Wang, L.; et al. Factors Influencing the Uptake and Speciation Transformation of Antimony in the Soil-Plant System, and the Redistribution and Toxicity of Antimony in Plants. *Sci. Total Environ.* **2020**, *738*, 140232.
3. Long, J.; Tan, D.; Deng, S.; et al. Antimony Accumulation and Iron Plaque Formation at Different Growth Stages of Rice (*Oryza sativa* L.). *Environ. Pollut.* **2019**, *249*, 414–422.
4. Ren, J.; Ma, L.Q.; Sun, H.; et al. Antimony Uptake, Translocation and Speciation in Rice Plants Exposed to Antimonite and Antimonate. *Sci. Total Environ.* **2014**, *475*, 83–89.
5. Deng, J.; Xiao, T.; Fan, W.; et al. Relevance of the Microbial Community to Sb and As Biogeochemical Cycling in Natural Wetlands. *Sci. Total Environ.* **2022**, *818*, 151826.
6. Hao, C.; Sun, X.; Peng, Y.; et al. Geochemical Impact of Dissolved Organic Matter on Antimony Mobilization in Shallow Groundwater of the Xikuangshan Antimony Mine, Hunan Province, China. *Sci. Total Environ.* **2023**, *860*, 160292.
7. Wu, T.; Zhang, N.; Liu, C.; et al. Factors Driving Antimony Accumulation in Soil-Pakchoi and Wheat Agroecosystems: Insights and Predictive Models. *Environ. Pollut.* **2024**, *351*, 124016.
8. Pan, W.; Zou, Q.; Hu, M.; et al. Microbial Community Composition and Co-Occurrence Patterns Driven by Co-Contamination of Arsenic and Antimony in Antimony-Mining Area. *J. Hazard. Mater.* **2023**, *454*, 131535.
9. Yu, H.; Liu, S.; Weng, W.; et al. Generational Specific Recruitment of Arsenic- and Antimony-Reducing Microorganisms in Plant Root-Associated Niches for Adapting to Metalloid-Metal Pollution. *Environ. Sci. Technol.* **2024**, *58*, 19567–19578.
10. Tang, S.; Song, X.; Chen, J.; et al. Widespread Distribution of the *arsO* Gene Confers Bacterial Resistance to Environmental Antimony. *Environ. Sci. Technol.* **2023**, *57*, 14579–14588.
11. Liu, B.; Yao, J.; Chen, Z.; et al. Biogeography, Assembly Processes and Species Coexistence Patterns of Microbial Communities in Metalloids-Laden Soils around Mining and Smelting Sites. *J. Hazard. Mater.* **2022**, *425*, 127945.
12. Wang, N.; Wang, A.; Xie, J.; et al. Responses of Soil Fungal and Archaeal Communities to Environmental Factors in an Ongoing Antimony Mine Area. *Sci. Total Environ.* **2019**, *652*, 1030–1039.
13. Li, B.; Xu, R.; Sun, X.; et al. Microbiome–Environment Interactions in Antimony-Contaminated Rice Paddies and

the Correlation of Core Microbiome with Arsenic and Antimony Contamination. *Chemosphere* **2021**, *263*, 128227.
14. Lin, H.; Qin, K.; Dong, Y.; et al. A Newly-Constructed Bifunctional Bacterial Consortium for Removing Butyl Xanthate and Cadmium Simultaneously from Mineral Processing Wastewater: Experimental Evaluation, Degradation and Biomineralization. *J. Environ. Manage.* **2022**, *316*, 115304.
15. Bararunyeretse, P.; Zhang, Y.; Ji, H. Molecular Biology-Based Analysis of the Interactive Effect of Nickel and Xanthates on Soil Bacterial Community Diversity and Structure. *Sustainability* **2019**, *11*, 3888.
16. Li, H.; Yao, J.; Min, N.; et al. New Insights on the Effect of Non-Ferrous Metal Mining and Smelting Activities on Microbial Activity Characteristics and Bacterial Community Structure. *J. Hazard. Mater.* **2023**, *453*, 131301.
17. Luo, Y.; Xing, R.; Wan, Z.; et al. Vertical Distribution of Nutrients, Enzyme Activities, Microbial Properties, and Heavy Metals in Zinc Smelting Slag Site Revegetated with Two Herb Species: Implications for Direct Revegetation. *Sci. Total Environ.* **2023**, *879*, 163206.
18. Zhao, X.; Huang, J.; Lu, J.; et al. Study on the Influence of Soil Microbial Community on the Long-Term Heavy Metal Pollution of Different Land Use Types and Depth Layers in Mine. *Ecotoxicol. Environ. Saf.* **2019**, *170*, 218–226.
19. Li, Y.; Zhang, M.; Xu, R.; et al. Arsenic and Antimony Co-Contamination Influences on Soil Microbial Community Composition and Functions: Relevance to Arsenic Resistance and Carbon, Nitrogen, and Sulfur Cycling. *Environ. Int.* **2021**, *153*, 106522.
20. Li, Y.; Lin, H.; Gao, P.; et al. Synergistic Impacts of Arsenic and Antimony Co-Contamination on Diazotrophic Communities. *Microb. Ecol.* **2022**, *84*, 44–58.
21. Sun, W.; Sun, X.; Li, B.; et al. Bacterial Response to Sharp Geochemical Gradients Caused by Acid Mine Drainage Intrusion in a Terrace: Relevance of C, N, and S Cycling and Metal Resistance. *Environ. Int.* **2020**, *138*, 105601.
22. Li, Y.; Guo, L.; Haggblom, M.M.; et al. *Serratia* spp. Are Responsible for Nitrogen Fixation Fueled by As(III) Oxidation, a Novel Biogeochemical Process Identified in Mine Tailings. *Environ. Sci. Technol.* **2022**, *56*, 2033–2043.
23. Liang, J.L.; Liu, J.; Jia, P.; et al. Novel Phosphate-Solubilizing Bacteria Enhance Soil Phosphorus Cycling Following Ecological Restoration of Land Degraded by Mining. *ISME J.* **2020**, *14*, 1600–1613.
24. Zou, Q.; An, W.; Wu, C.; et al. Red Mud-Modified Biochar Reduces Soil Arsenic Availability and Changes Bacterial Composition. *Environ. Chem. Lett.* **2018**, *16*, 615–622.
25. Zou, Q.; Wei, H.; Chen, Z.; et al. Soil Particle Size Fractions Affect Arsenic (As) Release and Speciation: Insights into Dissolved Organic Matter and Functional Genes. *J. Hazard. Mater.* **2023**, *443*, 130100.
26. Huang, D.; Zhou, L.; Fan, H.; et al. Responses of Aggregates and Associated Soil Available Phosphorus, and Soil Organic Matter in Different Slope Aspects, to Seasonal Freeze-Thaw Cycles in Northeast China. *Geoderma* **2021**, *402*, 115184.
27. Wu, Z.; Yang, X.; Huang, L.; et al. *In Situ* Enrichment of Sulphate-Reducing Microbial Communities with Different Carbon Sources Stimulating the Acid Mine Drainage Sediments. *Sci. Total Environ.* **2023**, *898*, 165584.
28. Filella, M.; Belzile, N.; Chen, Y.-W. Antimony in the Environment: A Review Focused on Natural Waters I. Occurrence. *Earth Sci. Rev.* **2002**, *57*, 125–176.
29. Wilson, S.C.; Lockwood, P.V.; Ashley, P.M.; et al. The Chemistry and Behaviour of Antimony in the Soil Environment with Comparisons to Arsenic: A Critical Review. *Environ. Pollut.* **2010**, *158*, 1169–1181.
30. Leuz, A.-K.; Johnson, C.A. Oxidation of Sb(III) to Sb(V) by $O_2$ and $H_2O_2$ in Aqueous Solutions. *Geochim. Cosmochim. Acta* **2005**, *69*, 1165–1172.
31. Li, J.; Zheng, Q.; Liu, J.; et al. Bacterial-Fungal Interactions and Response to Heavy Metal Contamination of Soil. *Front. Microbiol.* **2024**, *15*, 1395154.
32. Zeng, K.; Huang, X.; Guo, J.; et al. Microbial-Driven Mechanisms for the Effects of Heavy Metals on Soil Organic Carbon Storage: A Global Analysis. *Environ. Int.* **2024**, *190*, 108467.
33. Zhao, X.; Huang, J.; Zhu, X.; et al. Ecological Effects of Heavy Metal Pollution on Soil Microbial Community Structure and Diversity on both Sides of a River around a Mining Area. *Int. J. Environ. Res. Public. Health.* **2020**, *17*, 5680.
34. Chen, Q.; Ding, J.; Zhu, D.; et al. Rare Microbial Taxa as the Major Drivers of Ecosystem Multifunctionality in Long-Term Fertilized Soils. *Soil Biol. Biochem.* **2020**, *141*, 107686.
35. Gong, Y.; Yang, S.; Chen, S.; et al. Soil Microbial Responses to Simultaneous Contamination of Antimony and Arsenic in the Surrounding Area of an Abandoned Antimony Smelter in Southwest China. *Environ. Int.* **2023**, *174*, 107897.
36. Philippot, L.; Chenu, C.; Kappler, A.; et al. The Interplay between Microbial Communities and Soil Properties. *Nat. Rev. Microbiol.* **2024**, *22*, 226–239.
37. Okkenhaug, G.; Zhu, Y.; He, J.; et al. Antimony (Sb) and Arsenic (As) in Sb Mining Impacted Paddy Soil from Xikuangshan, China: Differences in Mechanisms Controlling Soil Sequestration and Uptake in Rice. *Environ. Sci. Technol.* **2012**, *46*, 3155–3162.
38. Yin, Y.; Wang, X.; Hu, Y.; et al. Soil Bacterial Community Structure in the Habitats with Different Levels of Heavy Metal Pollution at an Abandoned Polymetallic Mine. *J. Hazard. Mater.* **2023**, *442*, 130063.
39. Diepens, N.J.; Dimitrov, M.R.; Koelmans, A.A.; et al. Molecular Assessment of Bacterial Community Dynamics and Functional End Points during Sediment Bioaccumulation Tests. *Environ. Sci. Technol.* **2015**, *49*, 13586–13595.
40. Fakhar, A.; Gul, B.; Gurmani, A.R.; et al. Heavy Metal Remediation and Resistance Mechanism of *Aeromonas*, *Bacillus*, and *Pseudomonas*: A Review. *Crit. Rev. Environ. Sci. Technol.* **2022**, *52*, 1868–1914.
41. Yin, K.; Lv, M.; Wang, Q.; et al. Simultaneous Bioremediation and Biodetection of Mercury Ion through Surface Display of Carboxylesterase E2 from *Pseudomonas aeruginosa* PA1. *Water Res.* **2016**, *103*, 383–390.

42. Reichman, S.M. Probing the Plant Growth-Promoting and Heavy Metal Tolerance Characteristics of *Bradyrhizobium japonicum* CB1809. *Eur. J. Soil Biol.* **2014**, *63*, 7–13.
43. Chen, X.; Wang, J.; Pan, C.; et al. Metagenomic Analysis Reveals the Response of Microbial Community in River Sediment to Accidental Antimony Contamination. *Sci. Total Environ.* **2022**, *813*, 152484.
44. Sun, W.; Sun, X.; Li, B.; et al. Bacterial Response to Antimony and Arsenic Contamination in Rice Paddies during Different Flooding Conditions. *Sci. Total Environ.* **2019**, *675*, 273–285.
45. He, Q.; Liu, Y.; Wan, D.; et al. Enhanced Biological Antimony Removal from Water by Combining Elemental Sulfur Autotrophic Reduction and Disproportionation. *J. Hazard. Mater.* **2022**, *434*, 128926.